Assignment of Electronic Transitions and Electron−Phonon Coupling of Er^{3+} Doped into Y_2O_3

Peter A. Tanner,* Xianju Zhou, and Fengyi Liu

Department of Biology and Chemistry, City University of Hong Kong, Tat Chee Avenue, Kowloon, Hong Kong S.A.R., People's Republic of China

Received: August 22, 2004; In Final Form: October 1, 2004

The assignments of bands in the electronic spectra of Y_2O_3:Er^{3+} to Er^{3+} ions situated at S_6 symmetry sites (Silver, J.; Martinez-Rubio, M. I.; Ireland, T. G.; Withnall, R. *J. Phys. Chem. B* **2001**, *105*, 7200; Silver, J.; Martinez-Rubio, M. I.; Ireland, T. G.; Fern, G. R.; Withnall, R. *J. Phys. Chem. B* **2001**, *105*, 948) are shown to be incorrect, and some of the conceptual errors in these works are also corrected. For example, the emission bands assigned to $^2H_{11/2} \rightarrow {}^4I_{15/2}$ transitions at S_6 sites are reassigned to $^2P_{3/2} \rightarrow {}^4I_{11/2}$ transitions of Er^{3+} at C_2 sites. In fact, all of the visible and ultraviolet bands can be assigned to Er^{3+} ions situated at C_2 sites. The optical spectra are remarkably complete and uncluttered from vibronic structure, except for emission transitions to the two highest ground-state crystal field levels, where the multiple structures are assigned to electron−phonon coupling effects.

1. Introduction

There continues to be a strong interest and further developments in the luminescence of the well-established phosphor Y_2O_3 doped with Er^{3+} (for example, refs 1−10). This host lattice crystallizes in the cubic space group $Ia3$ (T_h^7), and the Er^{3+} ions have two distinct sites available in which to substitute the host Y^{3+} ions without charge compensation. These are both six-coordinate and possess S_6 ($\equiv C_{3i}$) and C_2 site point group symmetry,[11] but the site occupation ratio is $3C_2$:$1S_6$. The electronic spectra and energy levels of Er^{3+} at the C_2 sites in Y_2O_3 up to about 34 000 cm^{-1} have long been established.[12] Moreover, the pure electronic transitions for Er^{3+} ions at S_6 sites are electric dipole (ED) forbidden and no previous reports have been made of such bands. Although these features may possess magnetic dipole intensity, they are expected to be generally much weaker than the ED allowed transitions of Er^{3+} at the C_2 symmetry site in the visible and ultraviolet regions.

It was therefore surprising that two recent publications in this journal[13,14] have assigned a number of strong bands in the electronic emission spectra of Y_2O_3:Er^{3+} to emission from Er^{3+} ions at S_6 sites from the temperature dependence of the spectra. In this study we show that the arguments for these assignments are flawed and the assignments are incorrect. All of the features in the visible and ultraviolet emission spectra can be assigned to Er^{3+} ions at C_2 sites. We also comment upon ground-state electron−phonon coupling effects.

2. Experimental Section

Chemical Preparation. The conventional nitrate−citrate sol−gel method was used to prepare Y_2O_3:Er^{3+} in the Y:Er ratios of 0.1, 0.5, 1.0, and 10 at. %. Y_2O_3 (99.999%, Aldrich) and Er_2O_3 (99.999%, Int. Lab., USA) were dissolved in concentrated HNO_3 (Riedel-de-Haën, 65%, analytical reagent), and the solution was taken to dryness. The residue was dissolved and the operation was repeated a further three times. Citric acid was then added (mole ratio of metal ions:citric acid of 1:3). After gentle warming, the resulting gel was dried at 110 °C and then fired twice at 1100 °C, with grinding prior to each firing.

Characterization of Physical Properties. The characterization of the powders by X-ray diffraction showed that they corresponded to the cubic-type Y_2O_3 structure. Visible region absorption spectra (resolution 2 cm^{-1}) were recorded at temperatures between 295 and 20 K using pressed disks of Y_2O_3:Er^{3+} (10−30 at. %) with 10% w/w NaCl, using a Fiberlite source and an Acton 0.5 monochromator equipped with a charge-coupled detector. The samples were housed in an Oxford Instruments closed-cycle cryostat. Emission spectra were taken for powders pressed into the copper slots of the sample holder, using an air-cooled Ar^+ laser (Omnichrome) or a Panther optical parametric oscillator pumped by the second harmonic of a Surelite Nd:YAG laser.

3. Results and Discussion

In this section we first provide comments concerning some of the rationale and reasoning given in refs 13 and 14. Then, we pinpoint two examples of the incorrect assignments to the S_6 sites therein. The $^4I_{15/2}$ ground-state energy levels of Er^{3+} in Y_2O_3 are established herein from the previously unpublished (to our knowledge) $^4S_{3/2}$ low temperature emission spectrum, and are in agreement with early studies.[15,16] Then these energy levels are used in the interpretation of the room temperature and low temperature absorption spectra in the region between 542 and 518 nm (18 450−19 300 cm^{-1}), where features have been assigned to S_6 site emission in Y_2O_3:Er^{3+},Yb^{3+}. However, it is also necessary to investigate the emission from $^2P_{3/2}$ in order to solve the problem of the anomalous temperature dependence which was raised in ref 13. The presence of Yb^{3+} in the Y_2O_3:Er^{3+} samples does not give noticeable line shifts or intensity changes *within* the multiplet to multiplet transitions, and the relevant line positions in the absorption and emission spectra are coincident for a given sample.

Some of the energy levels of Er^{3+} in Y_2O_3 are shown in Figure 1; the $^{2S1+}L_J$ multiplet terms are labeled Z for the

10.1021/jp046217n CCC: $27.50
Published on Web 11/26/2004

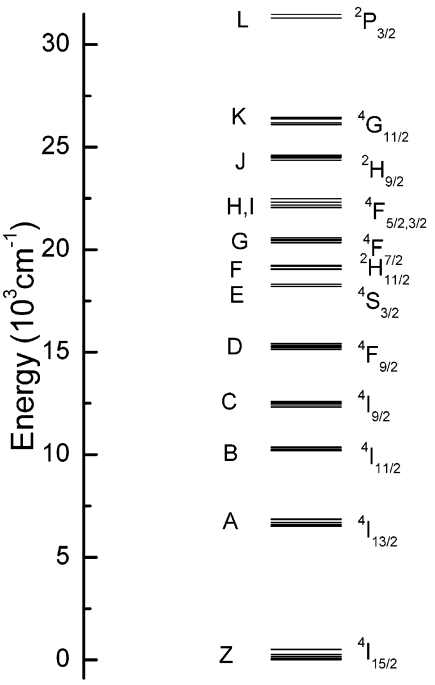

Figure 1. Some energy levels of Er^{3+} in Y_2O_3:Er^{3+}.

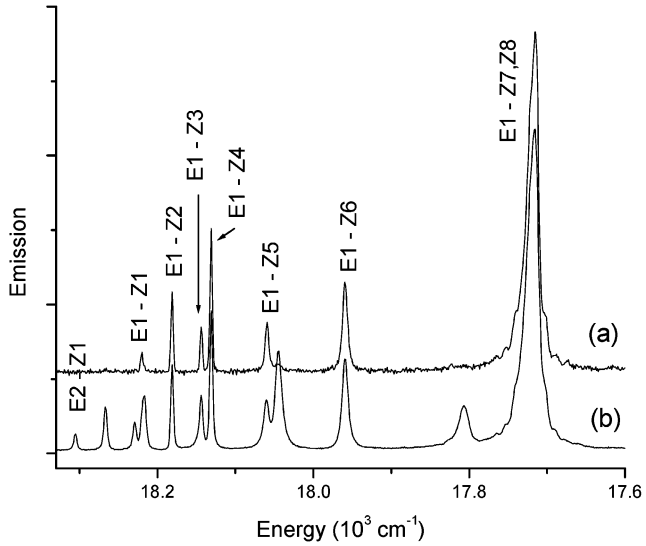

Figure 2. Emission spectra of Y_2O_3:Er^{3+} (0.5 at. %): (a) 514 nm excitation at 10 K; (b) 488 nm excitation at 50 K. $^4S_{3/2}$ levels E1 and E2 are at 18 210 and 18 315 cm^{-1}, respectively; $^4I_{15/2}$ levels Z1, Z2, Z3, Z4, Z5, and Z6 are at 0, 39, 77, 89, 160, and 260 cm^{-1}, respectively, with Z7, Z8 ~500 cm^{-1}. The relative intensities of (a) and (b) are arbitrary. The assignments of the remaining bands in (b) to E2 are analogous to those for E1.

TABLE 1: Assignment of Bands in the Room Temperature $^2P_{3/2} \rightarrow {}^4I_{11/2}$ Emission Transition of Er^{3+} in Y_2O_3 from the Spectrum in Ref 14, Figure 8[a]

band no.	energy (cm^{-1})	assignment upper $^2P_{3/2}$−lower $^4I_{11/2}$
1	21 303mw	L2−B1
2	21 283m	L2−B2
3	21 255m	L2−B3
4	21 234m	L2−B4
5	21 138vw	L2−B5
6	21 113sh	L2−B6
7	21 100s	L1−B1
8	21 079mw	L1−B2
9	21 054s	L1−B3
10	21 035s	L1−B4
11	20 936s	L1−B5
12	20 921vs	L1−B6

[a] s, strong; m, medium; w, weak; v, very; sh, shoulder. The upper $^2P_{3/2}$ levels are (in cm^{-1}) L1 (31 289) and L2 (31 488).

electronic ground state, and thence A, B, C, ... in order of increasing energy. This diagram differs from those given in refs 13 and 14 in several respects. First, in Figure 1, all energy levels correspond solely to Er^{3+} at C_2 sites. In this site symmetry all crystal field states are Kramers doublets, with each J multiplet comprising $J + 1/2$ states. Since the two C_2 site point group symmetry representations do not carry information pertinent to the present study, the energy levels are labeled 1, 2, ... in order of increasing energy for the multiplet terms in Figure 1. All pure electronic transitions between these states are ED allowed at the C_2 symmetry site (see below). Second, the energies given in refs 13 and 14 do not correspond to multiplet term energies, but in some cases the energies correspond to the complete span of emission transitions, including the hot bands from a given multiplet term. In other cases the assignments are incorrect, such as those for $^4I_{11/2}$ (given as 11 834−11 337 cm^{-1}) and $^4F_{7/2}$ (given as 21 367−20 876 cm^{-1}). In ref 13 it is stated that some emission transitions span over 500 cm^{-1} so that "they are made up of overlap of more than one emission band". This is one of the two arguments in refs 13 and 14 for the assignment of emission transitions to Er^{3+} ions situated at *both* C_2 and S_6 sites, and it is incorrect. Since the crystal field splitting of the ground-state multiplet term $^4I_{15/2}$ is ~500 cm^{-1} (see below), the additional presence of hot transitions will then give rise to a span that is greater than this energy for transitions from excited multiplet terms to the ground state. This is because the hot transitions originate from higher crystal field levels of the excited multiplet term, typically split by several hundred cm^{-1}. It is important to recognize that the crystal field levels of a given multiplet term are in Boltzmann thermal equilibrium, so that the transition from each different excited crystal field state exhibits a different temperature dependence, characteristic of its energy difference above the lowest luminescent state of the given multiplet. Furthermore, luminescent states of different multiplet terms show different intensity−temperature behavior due to their distinctive nonradiative behaviors. The second argument in refs 13 and 14 for the assignments of spectral features to different symmetry sites relates to the different temperature dependences of these bands, and we reassign them all below to emission from Er^{3+} ions at C_2 sites.

Another point made in ref 13 is that the f-electron transitions are forbidden, "but the parity selection rule has been found to be broken most easily in oxides and oxysulfides where the configurational interaction between the 4f levels can occur." It is true that, to the first order parity selection rule, f^N−f^N pure electronic ED transitions are forbidden, but they become allowed by the mixing of f^N wave functions with antiparity ones (such as $f^{N-1}d$), and not with other f^N wave functions.[17] This mixing is possible at the C_2 site of Er^{3+} where there is no inversion symmetry.

Electronic Ground-State Assignments. We now consider the electronic ground-state crystal field energy assignments for Y_2O_3:Er^{3+}. Figure 2 shows the 10 and 50 K emission spectra of Y_2O_3:Er^{3+} (0.5 at. %) powder between 17 600 and 18 330 cm^{-1} under 514.5 and 488 nm excitation, respectively. Under 355 nm excitation, additional bands readily assigned to the $^2H_{9/2} \rightarrow {}^4I_{13/2}$ transition are observed in this region. Comparison of Figure 2 with the room temperature spectrum presented in ref 18 enables the ground-state assignments to be made as marked

TABLE 2: Bands in the $^2H_{11/2}-{}^4I_{15/2}$ Room Temperature Absorption and Emission Transitions of Er^{3+} in Y_2O_3

energy (cm^{-1})			assignment[a]	
	Figure 3			
ref 13[b]	band no.		upper $^2H_{11/2}-$ lower $^4I_{15/2}$	upper $^2P_{3/2}-$ lower $^4I_{11/2}$
19 247s	1	19 246	F6−Z1	
19 221vw	2	19 220	F5−Z1	
	3	19 208	F6−Z2	
19 194m	4	19 191	F4−Z1	
19 189w	5	19 185	F5−Z2	
19 169m	6	19 170	F6−Z3	L2−C1
19 157s	7	19 157	F6−Z4	
19 146s	8	19 148	F5−Z3; F4−Z2	
19 133s	9	19 135	F5−Z4	
19 116m	10	19 117	F4−Z3	
19 104ms	11	19 104	F4−Z4	
19 076	12	19 077	F3−Z1	
19 050w	13	19 049	F2−Z1	
19 039ms	14	19 040	F1−Z1; F3−Z2	
19 012sh	15	19 013	F2−Z2	
19 003s	16	19 004	F3−Z3; F1−Z2	
18 986w	17	18 987	F3−Z4; F6−Z6	
18 973m	18	18 976	F2−Z3	L1−C1
18 961w	19	18 963	F2−Z4; F1−Z3; F5−Z6	
18 955m	20	18 957	F1−Z4	
18 931vw	21	18 932	F4−Z6	
18 920w	22	18 920	F3−Z5	L2−C4
18 890w	23	18 892	F2−Z5	L2−C5
18 860w				L1−C2
18 815vw	24	18 815	F3−Z6	
18 787m	25	18 788	F2−Z6	L1−C3
18 721mw	26	18 723	F5−Z7, Z8	L1−C4
18 692m	27	18 692	F4−Z7, Z8	L1−C5
18 578s	28	18 576	F3−Z7, Z8	
18 543s	29	18 546	F2−Z7, Z8	

[a] Due to small concentration shifts and calibration differences, band 1 in our spectrum has been placed at the same energy as band 1 in ref 13, and all other bands were shifted by this same energy difference. The upper $^2H_{11/2}$ levels are labeled F1−F6 (with energies given by the transitions to Z1), and the ground-state $^4I_{15/2}$ levels, as deduced from Figure 1, are Z1−Z8. From the analysis, the upper $^2P_{3/2}$ levels are (in cm^{-1}) L1 (31 289) and L2 (31 488); and the lower $^4I_{9/2}$ levels are C1−C5, in cm^{-1}: C1 (12 318), C2 (12 429), C3 (12 506), C4 (12 569), and C5 (12 597), which show a systematic calibration difference of ~6 cm^{-1} from the energies given in ref 12. [b] These energies were measured from the hard copy spectrum in Figure 8 of ref 13 and are not corrected to vacuum. The descriptive letters are explained in the footnote to Table 1. Bands in italics are those in ref 13 that were assigned to emission from Er^{3+} at S_6 site symmetry.

in the figure, with Z1−Z8 representing the $^4I_{15/2}$ crystal field levels. The levels Z7 and Z8 are not clearly identified in Figure 2, and we take a mean value of ~500 cm^{-1} for these two close energy levels (see below). Our study of the $^4I_{11/2}$, $^4I_{9/2}$, $^4F_{9/2} \rightarrow {}^4I_{15/2}$ emission transitions provides identical assignments of the ground-state energy levels, with all bands being associated with Er^{3+} at C_2 sites. Furthermore, from our absorption and emission spectra, we assign the $^4I_{9/2}$ energy levels (labeled C1−C5) to the same crystal field splittings as in ref 12.

Reassignment of Emission Bands between 467.5 and 480 nm. The 12 emission bands between 467.5 and 480 nm (21 390 and 20 830 cm^{-1}) at room temperature were assigned to the $^4F_{7/2} \rightarrow {}^4I_{15/2}$ transition in ref 13, and then reassigned in ref 14 to emission from both S_6 and C_2 sites of the $^4F_{3/2} \rightarrow {}^4I_{15/2}$ transition. In fact, these bands correspond to the $^2P_{3/2} \rightarrow {}^4I_{11/2}$ transition at only the C_2 site. The assignments are collected in Table 1, from our measurements (±4 cm^{-1}) of the hard copy spectrum, Figure 8. From the analysis, the two $^2P_{3/2}$ levels are located at (in cm^{-1}) L1 (31 289) and L2 (31 488). The six $^4I_{11/2}$ energies are located in agreement with the energies from our absorption spectra and also those in ref 12.

Reassignment of Emission Bands between 542 and 518 nm. Now we may consider the region between 542 and 518 nm (18 450 and 19 305 cm^{-1}) of the emission spectrum of Y_2O_3:Er^{3+}, as depicted in ref 13, corresponding to the $^2H_{11/2} \rightarrow {}^4I_{15/2}$ emission spectrum. We tabulate the band energies in column 1 of Table 2, as we measured from the hard copy of the spectrum in ref 13. Figure 3a shows the room temperature absorption spectrum of a NaCl disk containing Y_2O_3:Er^{3+} in the same spectral region, and the numbered bands are tabulated in columns 2 and 3 of Table 2. Assignments are presented in column 4. We have presented the data from absorption because the situation could possibly arise in emission that energy transfer occurs from Er^{3+} ions at S_6 sites to those at C_2 sites, so that the S_6 bands would then not show. In absorption, however, if bands are present for Er^{3+} at S_6 sites, then they would appear. As is evident from Table 2, the room temperature absorption bands coincide with the emission bands reported in refs 13 and 14. The energies of excited crystal field levels of $^2H_{11/2}$ (labeled F1−F6) and $^4I_{15/2}$ (Z1−Z8) are in agreement with refs 12, 15, and 16 and with the values from Figure 2.

One band is clearly visible in the spectrum at 18 860 cm^{-1} in ref 13 (Figure 8) but is not present in Figure 3 herein (or in our 514.5 nm room temperature emission spectrum of the 0.5 at. % Er^{3+} doped sample), and cannot be assigned to the transition between $^2H_{11/2}$ and $^4I_{15/2}$. It would be easy to discount this one band as an artifact, but it is not. In fact, it corresponds to emission from $^2P_{3/2}$, and not from $^2H_{11/2}$. The other emission bands from $^2P_{3/2}$ are, by coincidence, overlapped by features in the $^2H_{11/2} \rightarrow {}^4I_{15/2}$ transition. The assignments are collected for the $^2P_{3/2} \rightarrow {}^4I_{9/2}$ transition in the final column of Table 2, and we can then understand why these bands were associated with the anomalous temperature dependence in ref 13 (i.e., these bands correspond to the italicized ones in column 1 of Table 2). The reason is not concerned with the different C_2 or S_6 sites, but with the different luminescent state: $^2P_{3/2}$ versus $^2H_{11/2}$. It is interesting that $^2P_{3/2}$ is populated at room temperature by 632.8 nm radiation, although Vetrone et al. have also achieved this using 980 nm radiation.[1]

TABLE 3: Displacement Energies of Bands (in cm^{-1}: Relative to Zero Phonon Lines) in the Z7 and Z8 Regions of $^4S_{3/2}$ and $^4F_{9/2} \rightarrow {}^4I_{15/2}$ Emission Spectra of Y_2O_3:Er^{3+} at ~10 K under Different Excitation Lines (Figure 4)

Figure 4a	displacement	Figure 4b	displacement	Figure 4c	displacement	phonon combinations[a]
8	454	8	456			Z3 + 381
7	466	7	464, 469	7	464	Z4 + 381, Z1 + 82 + 381
6	478	6	478	6	479	Z2 + 434
5	497	5	498	5	497	Z7, Z5 + 334
4	504	4	505	4	503	Z8, Z3 + 434
3	518	3	519	3	519	Z2 + 473, Z1 + 381 + 133, Z1 + 320 + 196
2	530	2	532	2	531	Z1 + 334 + 196
1	547	1	546	1	543	Z5 + 381, Z1 + 381 + 164

[a] Raman phonons from ref 20.

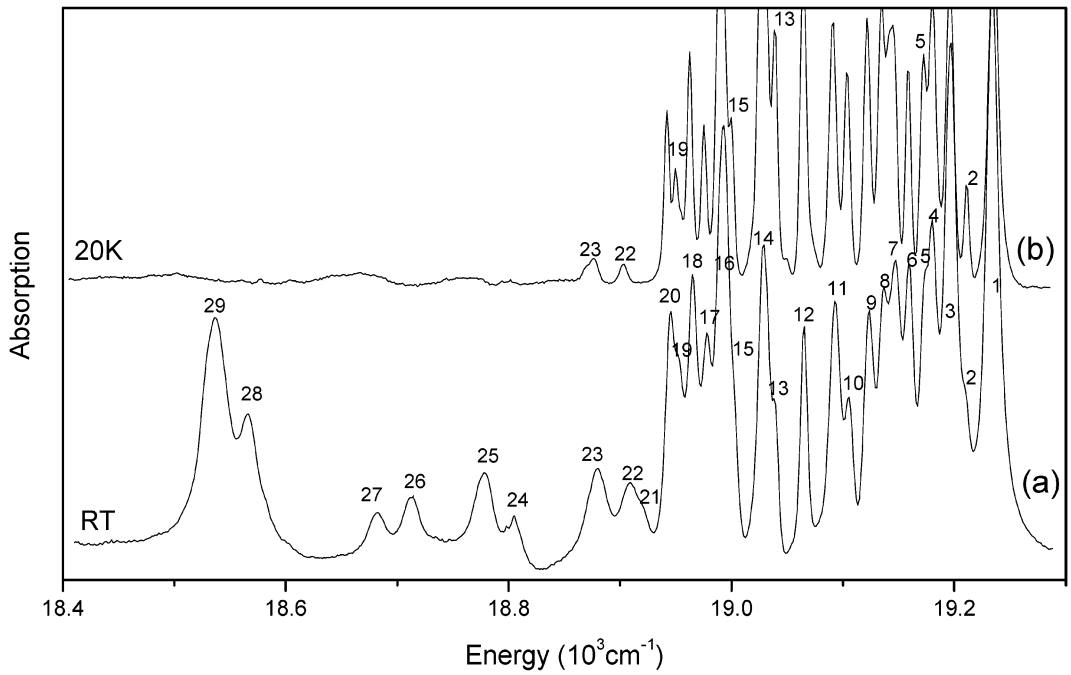

Figure 3. Room temperature (a) and 20 K (b) absorption spectra of Y_2O_3:Er^{3+} (10 at. %) mixed 10% w/w with NaCl and pressed into a disk. (Band numbers refer to Table 2.)

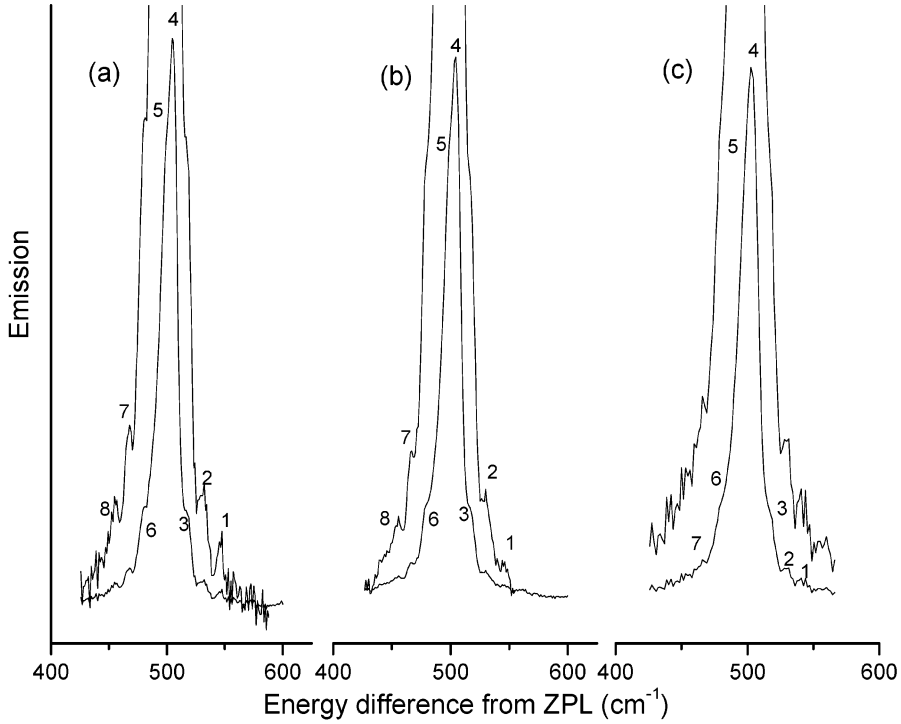

Figure 4. Bands in the Z7 and Z8 regions of $^4S_{3/2}$ and $^4F_{9/2} \rightarrow {}^4I_{15/2}$ emission spectra of Y_2O_3:Er^{3+} at ~10 K under different excitation lines. (a) E1 → Z7, Z8, 514 nm excitation, 0.1 at. % Er^{3+}; (b) E1 → Z7, Z8, 514 nm excitation, 0.5 at. % Er^{3+}; (c) D1 → Z7, Z8, 488 nm excitation, 0.1 at. % Er^{3+}. The zero phonon lines E1 and D1 are at 18 210 and 15 102 cm^{-1}, respectively. (Band numbers refer to Table 3.)

Electron−Phonon Coupling. Finally, we comment on an interesting observation from our present emission study of Y_2O_3:Er^{3+}. Figure 4 shows in detail emission bands corresponding to transitions terminating on the Z7 and Z8 ground-state levels. Our spectra are not highly resolved because the temperature is ~10 K and we employed powder samples rather than single crystals. Nevertheless, instead of just two bands in each case, there are many weaker features surrounding the stronger two components at 497 and 504 cm^{-1}. The bands are similar under different excitation wavelengths, and are not due to defects (i.e., they do not change under different excitation lines), artifacts due to the superposition of absorption bands (i.e., the bands are similar for different emission transitions), isotope effects (the splittings are too large), or ion−ion interactions (i.e., the relative intensities are independent of concentration in the range studied from 0.1 to 1 at. % Er^{3+}). These features are assigned to electron−phonon coupled states. The energies of the features from the luminescence spectrum, relative to the zero phonon line energies, are included in Table 3, with bands numbered as in Figure 4. The $k = 0$ infrared and Raman spectra are available

for several lanthanide sesquioxides.[19,20] The phonon modes that couple to the electronic states are the linear combinations of unit cell modes that transform at the C_2 site of Er^{3+}. However, we show in Table 3 (final column) the fact that, even from the Raman data for Y_2O_3:Er^{3+},[20] there are many phonon combinations that produce energies close to those of the vibronic bands between 450 and 550 cm^{-1}. These numbers are purely illustrative and incomplete and are not intended as rigorous assignments since the details of the resonance phenomena are unknown. However, this serves to show that multiple bands appear in the region near 500 cm^{-1} above the ground state, whereas other ground-state levels are not split, because (i) many resonant phonon combinations are possible for the former—either 2-phonon or phonon plus excited ground-state level—and (ii) the phonons are internal modes that are flat and have a high density in *k*-space.

4. Conclusions

The main purpose of this work has been to show that the visible and ultraviolet emission spectra of Y_2O_3:Er^{3+} can be interpreted as from Er^{3+} situated at C_2 sites. The spectra are very beautiful (even for a powder sample), are complete and well-resolved, and are virtually free of vibronic structure (with the exception of the Z7 and Z8 bands). The temperature behavior of different emission bands within a particular group has enabled the clear identification of transitions from initial luminescent states which are (i) different crystal field states of the same multiplet and (ii) different multiplet terms. There is also a lesson that every spectral feature must be accounted for to gain a complete understanding. The assignments given in column 4 of Table 2 for the $^2H_{11/2}-^4I_{15/2}$ group of bands in ref 13 would appear to be complete. However, by neglecting the weak feature at 18 860 cm^{-1}, the real reason for the anomalous temperature discussed in ref 13 would not then be apparent.

We consider that it is unnecessary to give reassignments for all the other reported S_6 site emissions in refs 13 and 14. The C_2 site energy levels for this system are already available in ref 12.

Acknowledgment. This research was supported by the City University Strategic Research Grant 7001459.

References and Notes

(1) Vetrone, F.; Boyer, J. C.; Capobianco, J. A.; Speghini, A.; Bettinelli, M. *Chem. Mater*. **2003**, *15*, 2737.

(2) Vetrone, F.; Boyer, J. C.; Capobianco, J. A.; Speghini, A.; Bettinelli, M. *J. Phys. Chem. B* **2003**, *107*, 1107.

(3) Redmond, S.; Rand, S. C.; Ruan, X. L.; Kaviany, M. *J. Appl. Phys*. **2004**, *95*, 4069.

(4) Kim Anh, T.; Quoc Minh, L.; Vu, N.; Thu Huong, T.; Thanh Huong, N.; Barthou, C.; Strek, W. *J. Lumin.* **2003**, *102−103*, 391.

(5) Auzel, F.; Baldacchini, G.; Laversenne, L.; Boulon, G. *Opt. Mater*. **2003**, *24*, 103.

(6) Laversenne, L.; Goutaudier, C.; Guyot, Y.; Cohen-Adad, M. Th.; Boulon, G. *J. Alloys Compd.* **2002**, *341*, 214.

(7) Georgobiani, A. N.; Gruzintsev, A. N.; Nikiforova, T. V.; Barthou, C.; Benalloul, P. *Inorg. Mater.* **2002**, *38*, 1199.

(8) Matsuura, D. *Appl. Phys. Lett*. **2002**, *81*, 4526.

(9) Korzenski, M. B.; Lecoeur, P.; Mercey, B.; Camy, P.; Doualan, J. L. *Appl. Phys. Lett.* **2001**, *78*, 1210.

(10) Capobianco, J. A.; Vetrone, F.; D'Alesio, T.; Tessari, G.; Speghini, A.; Bettinelli, M. *Phys. Chem. Chem. Phys*. **2000**, *2*, 3203.

(11) Faucher, M.; Pannetier, J. *Acta Crystallogr., Sect. B* **1980**, *36*, 3209.

(12) Morrison, C. A.; Leavitt, R. P. *Handbook on the Physics and Chemistry of Rare Earths*; Gschneidner, K. A., Jr., Eyring, L., Eds.; North-Holland Publishing Co.: Amsterdam, 1982; Chapter 46, p 569.

(13) Silver, J.; Martinez-Rubio, M. I.; Ireland, T. G.; Fern, G. R.; Withnall, R. *J. Phys. Chem. B* **2001**, *105*, 948.

(14) Silver, J.; Martinez-Rubio, M. I.; Ireland, T. G.; Withnall, R. *J. Phys. Chem. B* **2001**, *105*, 7200.

(15) Kisliuk, P.; Krupke, W. F.; Gruber, J. B. *J. Chem. Phys.* **1964**, *40*, 3606.

(16) Chang, N. C.; Gruber, J. B.; Leavitt, R. P.; Morrison, C. A. *J. Chem. Phys.* **1982**, *6*, 3877.

(17) Tanner, P. A. *Top. Curr. Chem.* **2004**, *241*, 167.

(18) Tanner, P. A.; Wong, K. L. *J. Phys. Chem. B* **2004**, *108*, 136.

(19) McDevitt, N. T.; Davidson, A. D. *J. Opt. Soc. Am.* **1966**, *56*, 1966.

(20) Schaack, G.; Koningstein, J. A. *J. Opt. Soc. Am.* **1970**, *60*, 1110.